Cancer Chemotherapy and Pharmacology (2019) 83:519–530
https://doi.org/10.1007/s00280-018-3755-9

ORIGINAL ARTICLE

Anti-liver cancer effect and the mechanism of arsenic sulfide in vitro and in vivo

Shudan Wang[1] · Chao Zhang[2] · Yumei Li[1] · Ping Li[1] · Dafang Zhang[1] · Chaoying Li[1]

Received: 20 July 2018 / Accepted: 4 December 2018 / Published online: 12 December 2018

Abstract

Purpose This study aimed at investigating the anti-tumor effect of arsenic sulfide (As_2S_2) against liver cancer both in vivo and in vitro and to elucidate its underlying mechanisms.

Methods Cell viability of the human hepatocellular carcinoma cell lines SMMC-7721, BEL-7402, HepG2 were measured by CCK-8 assay. The effects of As_2S_2 on cell proliferation and apoptosis of SMMC-7721 cells were investigated using Calcein-AM and PI staining, Hoechst 33258 staining, crystal violet staining, and JC-1 staining. Cell cycle and Annexin V/PI assay were analyzed via flow cytometry. The expression of apoptosis-related proteins, phosphorylation of PI3K and AKT were detected by Western blotting. H22-bearing mice model was established to evaluate the anti-tumor effect of As_2S_2 in vivo. HE staining, PCNA was observed via immunohistochemistry, and TUNEL assay was used to assess the anti-proliferation and pro-apoptotic effects of As_2S_2.

Results As_2S_2 significantly inhibited the growth of human hepatoma cells SMMC-7721, BEL-7402 and HepG2. As_2S_2 inhibited cell proliferation effectively by inducing G0/G1 cell cycle arrest in SMMC-7721 cells. As_2S_2 could increase Bax/Bcl-2 ratio, decrease mitochondrial membrane potential, promote the release of cytochrome *c*, increase the levels of cleaved caspase-3 and PARP, indicating that As_2S_2 induced apoptosis in SMMC-7721 cells via mitochondrial-mediated apoptosis pathway. Further research showed that As_2S_2 inhibited the PI3K/AKT signaling pathway leading to apoptotic cell death. In addition, As_2S_2 significantly inhibited tumor growth in H22-bearing mice and induced apoptosis by deactivating PI3K/AKT pathway, which was consistent with the in vitro results.

Conclusion These findings suggested that As_2S_2 could induce apoptosis of liver cancer cells in vitro and in vivo, which was related to PI3K/AKT-mediated mitochondrial pathway and may provide a novel promising therapeutic agent for liver cancer treatment.

Keywords Liver cancer · As_2S_2 · Apoptosis · SMMC-7721 cells · PI3K/AKT pathway

Introduction

Liver cancer has proved to be the most prevalent malignancy, mainly comprising hepatocellular carcinoma (HCC) and intrahepatic cholangiocarcinoma (iCCA). It is the second major cause of cancer-related death in the world, with highly aggressive and poor prognosis [1]. It is estimated that about 800,000 new cases and 700,000 deaths are associated with liver cancer worldwide every year [2]. Presently, surgical resection and liver transplantation remain the principal treatment options of early stage of liver cancer. However, only 10% of the patients have the possibility of complete hepatectomy [3]. The total survival rate of the patients with liver cancer is still poor. To date, there is no effective prevention and treatment for liver cancer patients; it is highly

Shudan Wang and Chao Zhang have contributed equally to this work.

✉ Dafang Zhang
zdf0431@126.com

✉ Chaoying Li
chaoying_li@126.com

[1] School of Pharmaceutical Sciences, Changchun University of Chinese Medicine, Changchun 130117, China

[2] School of Life Sciences, Beijing University of Chinese Medicine, Beijing 100029, China

desirable to develop more efficient agents to treat liver cancer and improve the quality of life of patients.

The development of liver cancer is believed to be correlated with dysregulation of apoptosis [4]. In 1972, Kerr, an Australian scholar, first proposed the concept of apoptosis. Apoptosis is a spontaneous, programmed cell death to remove damaged, dysfunctional, or superfluous cells, which is an indispensable process of adjustment and control for the living organisms [5, 6]. Apoptosis mainly involves two representative approaches: the extrinsic pathway and the intrinsic pathway. The extrinsic pathway is also called the death receptor-mediated pathway. The death receptor is a certain protein on the surface of the cell membrane, which can bind to specific ligands carrying apoptotic signals and rapidly transduce apoptotic signals into cells, thus inducing apoptosis [7]. The intrinsic pathway, also called the mitochondrial pathway, is mediated by the Bcl-2 family. Members of Bcl-2 family lead to the unfolding of the mitochondrial permeability transport pore (mPTP), the increase of membrane permeability and promote cytochrome *c* release, which is the key center in the regulation of apoptosis. Cytochrome *c* and caspase-9 precursors released into the cytoplasm and apoptosis activator Apaf-1 form apoptosomes, activate caspase-9 activation and subsequently trigger the caspase cascade activation. Poly ADP-ribose polymerase (PARP), which acts as a DNA damage receptor, is sheared and inactivated to lose its repair function, resulting in DNA fragmentation and chromatin condensation, ultimately, to apoptotic cell death [8, 9].

Previous researches have proved that phosphatidylinositol 3-kinase/protein kinase B (PI3K/AKT) signaling pathway is closely associated with the development and progression of human tumors and comes into a negative regulator status in apoptosis of tumor cells [10, 11]. AKT, a serine/threonine kinase, is the critical mediator of PI3K-initiated signaling and can promote the survival of tumor by up-regulating the Bcl-2 expression [12]. The Bcl-2 family plays a vital role of PI3K/AKT regulating apoptosis. Bcl-2 family refers to a class of evolutionarily conserved proteins that contain Bcl-2 homology (BH) domains, which is most prominent for their apoptosis regulation at the mitochondrion. Bcl-2 family is divided into two kinds of members, namely pro-apoptotic protein (such as Bax, Bid, Bad, Bik) and anti-apoptotic protein (such as Bcl-2, Bcl-XL, Bcl-w) [13]. As one of the principal pathways regulating Bcl-2 family proteins, PI3K/AKT regulates the phosphorylation level of Bcl-2 family proteins, affects the formation of its conformation or dimers and thus regulates apoptosis [14]. Therefore, inducing apoptosis of liver cancer cells will be an effective and highly active way for treating liver cancer and is a very significant index for exploring anticancer drugs.

For decades, traditional Chinese medicine (TCM) has shown impressive antineoplastic activity and has the distinguishing feature of lower drug resistance and higher safety. For example, the Curcuma wenyujin plant extract β-elemene has been widely used as an adjuvant therapeutic agent for cancer treatment including liver cancer in China [15]. In addition, researches have illustrated that TCM had preventive and therapeutic effects on liver cancer; several modern TCM preparations, such as Kanglaite, cinobufotalin and Ganfule, have been approved by the Chinese Pharmaceutical Administration for complementary treatment of liver cancer, and pharmacological actions and mechanisms of TCM are varied [16].

As three main types of arsenic compounds, arsenic trioxide (As_2O_3), arsenic sulfide (As_2S_2) and arsenic trisulfide (As_2S_3) have been extensively applied to TCM for over 3000 years [17]. As_2O_3 as a primary member of arsenic compound family has shown excellent therapeutic effect on acute promyelocytic leukemia, as well as for several solid tumors in clinical trials [18]. As_2S_2, the main ingredient of realgar, has gained more attention due to its advantages of easy oral intake, relative safety and sufficient resource [19]. Recent reports have indicated that As_2S_2 has been found to show strong suppressive anticancer effects in gastric cancer and osteosarcoma [20–24]. Nevertheless, little information about the underlying mechanisms for its anticancer activity is known.

In this research, we investigated the anti-tumor effect of As_2S_2 on human hepatoma SMMC-7721 cells, H22-bearing mice and underlying molecular mechanisms. It is expected that these results would provide a basis for the application of As_2S_2 in the treatment of liver cancer. We found, for the first time, that As_2S_2 induced apoptosis both in vivo and in vitro via mitochondrial pathway and PI3K/AKT signaling pathway in liver cancer.

Materials and methods

Cells and cell culture

Murine H22 hepatoma cells were kindly provided by Prof. Qin Fu (Jilin Cancer Institute). Human hepatocellular carcinoma cell lines SMMC-7721, BEL-7402 and HepG2 were purchased from Shanghai iCell Bioscience Inc. (Shanghai, China). Cells were maintained in RPMI 1640 or MEM medium including 10% fetal bovine serum and 100 units/mL penicillin–streptomycin (all from iCell Bio) and incubated at 37 °C in a humidified atmosphere of 5% CO_2.

Chemicals and reagents

As_2S_2 (purity of > 98%) was bought from Baoji Herbest Biotechnology (Baoji, Shanxi, China). The raw material solution at 10 mM was dissolved in 0.1 M NaOH, and the pH value was adjusted from 7.35 to 7.45 by HCl [20]. Next, the working solutions of As_2S_2 were diluted in the basal medium and stored at −20 °C in the dark. Cell counting kit (CCK-8), Calcein-acetoxymethyl ester (Calcein-AM) and propidium iodide

(PI) double stain kit, Hoechst 33258 staining kit, 5,5′,6,6′-Tetrachloro-1, 1′,3,3′-tetraethyl-imidacarbocyanine mitochondrial membrane potential assay kit (JC-1) were purchased from Yeasenbio (Shanghai, China). LY294002 and Annexin V-fluorescein isothiocyanate (FITC)/PI apoptosis detection kit were purchased from Beyotime (Nanjing, Jiangsu, China). Rabbit polyclonal antibodies against phosphorylated PI3K (p-PI3K/p85), AKT, p-AKT, Bcl-2, Bax, cytochrome *c*, cleaved caspase-3, PARP and β-actin, COX IV and horseradish peroxidase (HRP)-labeled secondary antibodies were bought from Wanleibio (Shenyang, Liaoning, China).

Cell viability assay

Cell viability was measured by CCK-8 assay in accordance with the manufacturer's instruction. Cells (5×10^3 cells/well, 100 µL) were plated into 96-well plates. SMMC-7721, BEL-7402 and HepG2 were treated with different As_2S_2 concentrations (0, 5, 10, 20, 30, 40 and 50 µM) for 24, 48 and 72 h. Absorbance at 450 nm was determined by an iMark Microplate reader (BioRad, California, USA). Complete culture medium without cells served as the blank group. The drug inhibitory concentration of 50% (IC_{50}) was determined through probability regression analysis.

$$\begin{aligned}\text{Cell viability} = \big(&\text{average OD of } As_2S_2\text{group}\\ &-\text{average OD of blank group}/\\ &\text{average OD of control group}\\ &-\text{average OD of blank group)} \times 100\%.\end{aligned}$$

Clone formation assay

SMMC-7721 cells (500 cells/well) were seeded into 6-well plates for 24 h, then incubated with different concentrations of As_2S_2 (12.5, 25 and 50 µM) for 24 h. Cells were recultured for another 14 days in As_2S_2-free conditions until cells grew into visible colonies. The culture medium was replaced every 3 days. Then, the cells were fixed in methanol, dyed in 0.1% crystal violet, and rinsed for 3 times with PBS. The number of clones over 50 cells were counted.

Calcein-AM/PI double staining and Hoechst 33258 staining

Observation of live and dead cells and the morphology of apoptotic cells by Calcein-AM/PI double fluorescent staining and Hoechst 33258 staining. SMMC-7721 cells (5×10^3 cells/well, 100 µL) plated into 96-well plates were treated with As_2S_2 (12.5, 25, 50 µM) for 24 h. Cells were then stained with 2 µM Calcein-AM and 4.5 µM PI or Hoechst 33258 (10 µg/mL) for 30 min in the dark at 37 °C. The number of live or apoptotic cells in three random fields was counted under IX73 fluorescence microscope (Olympus, Tokyo, Japan), and the results were expressed relative to the total number of cells.

Cell cycle assay

SMMC-7721 cells were seeded at a concentration of 5×10^4 cells/mL (4 mL) in 25 cm^2 flasks, after 24 h of attachment, incubated with or without As_2S_2 (12.5, 25 and 50 µM) for 24 h. Cells were collected by centrifugation, fixed in 70% ethanol, then washed in PBS and resuspended in 25 µL RNase and 10 µL PI, incubated in the dark at room temperature for 30 min. Cell cycle analysis was performed on Accuri C6 and the data were analyzed by Accuri C6 Software (Becton, Dickinson and Company, CA, USA).

Cell apoptosis assay

Cell apoptosis was examined by Annexin V-FITC/PI staining according to the manufacturer's instructions. Briefly, 2×10^5 cells were cultured in 25 cm^2 flasks for 24 h and manipulated with various concentrations of As_2S_2 (0, 12.5, 25 and 50 µM) for 24 h. Then, 2×10^4 cells were harvested and resuspended in 195 µL Annexin V binding buffer comprising 5 µL Annexin V-FITC and 10 µL PI for 15 min in the dark. Apoptotic rates were analyzed by Accuri C6 using Accuri C6 Software.

Mitochondrial membrane potential assay ($\Delta\Psi_m$)

JC-1 was applied to gauge mitochondrial membrane potential, which is a fluorescent lipophilic carbocyanine dye-sensitive detection of mitochondrial membrane potential changes in cells [25]. Cells (5×10^3 cells/well, 100 µL) were cultured in 96-well plates for 24 h and then incubated with or without As_2S_2 (0, 12.5, 25 and 50 µM) for 24 h. Cells were stained with JC-1 working solution in the dark at 37 °C for 20 min, washed with JC-1 binding buffer and placed in the medium. Fluorescence images were observed by IX73 fluorescence microscope (Olympus, Tokyo, Japan) and Image J version d 1.47 software (National Institutes of Health, Bethesda, USA) was used to quantify the green/red fluorescence intensity to indicate the change of mitochondrial membrane potential.

Western blot analysis

Western blot analysis was performed on SMMC-7721 cells from different groups, cells (1×10^6 cells/mL) were treated with or without As_2S_2 (0, 12.5, 25, 50 µM) for 24 h. Total proteins

were extracted using Radio Immunoprecipitation Assay lysis buffer containing 1% vol/vol phenylmethanesulfonyl fluoride (Wanleibio, Liaoning, China). The protein concentration of the whole lysates was determined by the BCA Protein Assay Kit (Wanleibio, Liaoning, China). Equivalent amounts of protein were loaded (40 μg/lane) and separated by sodium dodecyl sulfate-polyacrylamide gel electrophoresis and transferred to polyvinylidenefluoride membranes (Millipore, Billerica, MA, USA). 5% of the skimmed milk was used to seal the membranes and with specific primary antibodies (1:500) incubated overnight at 4 °C, then incubated with the corresponding horseradish peroxidase-conjugated goat anti-rabbit IgG secondary antibodies (1:5000). The target proteins were visualized with the enhanced chemiluminescence system (Wanleibio, Liaoning, China). The intensity of the target bands was quantified by Gel-Pro-Analyzer 4 (Media Cybernetics, Rockville, MD, USA).

Establishment of mice bearing H22 and treatments

All animal care and experimental procedures conformed to the Guidelines of the Care and Use of Laboratory Animals and were approved by the Institutional Ethics Committee of the Changchun University of Chinese Medicine. BALB/c SPF mice (female, 20 ± 2 g, 6-week-old) were bought from Changchun Institute of Biological Products (Changchun, Jilin, China) and maintained on standard chow and water. BALB/c mice were assigned to 5 groups with 8 mice in each group randomly.

H22 cells were resuspended in aseptic normal saline and injected into the abdominal cavity of BALB/c mice (4×10^6 cells per animal). Treatments were initiated 24 h after the injections of H22 cells. As_2S_2 (0.8, 1.6, 3.2 mg/kg) and 5-Fu (25 mg/kg, Jinyao, Tianjin, China) were intraperitoneally injected into the corresponding mice, respectively. The model group mice were given the equal volume of saline. Consistent treatment was given to the mice daily for 12 days. Mice weight was recorded every 2 days until animals were killed at day 13. Tumors were removed and weighed immediately. Each tumor was assigned to two parts in which one was fixed in 10% formaldehyde for histologic examination and immunohistochemistry, whereas the other stored at −80 °C for the analysis of Western blot.

$$\text{Tumor inhibition rate} = \left(1 - \left[\text{tumor weight in 5-Fu or } As_2S_2 \text{group} / \text{tumor weight in model group}\right]\right) \times 100\%.$$

Hematoxylin and eosin (HE) staining and immunohistochemistry assay

The tumor specimens of the mice were fixed with 10% formaldehyde for 24 h, paraffin embedded and cut into 5 μm-thick slices. For histologic examination, tissue slides were stained with hematoxylin and eosin (Solarbio, Beijing, China). For immunohistochemistry assay, tumor tissue sections were dewaxed, hydrated and antigen repaired. The slices were soaked in 3% H_2O_2 at room temperature for 15 min, then sealed with goat serum. The fixed tissue was incubated with primary antibodies against Proliferating cell nuclear antigen (PCNA, 1:100) overnight at 4 °C. Subsequently, the slices were subjected to biotin-labeled goat anti-rabbit IgG secondary antibody, horseradish enzyme labelling and DAB (all from Beyotime). Five separate fields were randomly selected in each slide and the average proportion of positive cells was assessed in each field.

TdT-mediated dUTP nick end labeling (TUNEL) assay

To measure apoptosis of tumor cells, we used TUNEL assay kit (Roche, Switzerland) according to the manufacturer's instructions. TUNEL-positive cells were observed and quantitatively analyzed under a DP73 microscope (Olympus, Japan).

Statistical analysis

Repeated experiments were conducted at least three times, and data were given as mean ± SD. For statistical analysis, one-way analysis of variance was performed for comparisons among groups using GraphPad Prism 7.0 version. (GraphPad Software, San Diego, CA, USA). $P<0.05$ was considered statistically significant.

Results

As_2S_2 inhibited the proliferation of SMMC-7721 cells

To investigate the anti-proliferative of As_2S_2, SMMC-7721, BEL-7402, HepG2 cells were incubated in As_2S_2 with concentrations from 5 to 50 μM for 24, 48 and 72 h, and cell viability was detected using CCK-8 assay. The results revealed that As_2S_2 significantly decreased the growth of SMMC-7721, BEL-7402, HepG2 cells in a dose-dependent manner, after As_2S_2 treatment for 24 h, the IC_{50} values were 25.63 ± 1.05, 28.99 ± 3.44 and 30.15 ± 3.43 μM, respectively (Fig. 1a). Since the SMMC-7721 cell line was the most susceptible to As_2S_2 treatment in the tested human hepatocellular carcinoma cell lines, we selected SMMC-7721 cell line for further research. Moreover, long-term exposure of SMMC-7721 cells to As_2S_2 led to an increased growth inhibitory effect, and colony formation assay showed that As_2S_2 could reduce colony numbers significantly (Fig. 1b, c). These results indicate that As_2S_2 showed strong anticancer activity on SMMC-7721 cells in vitro.

As_2S_2 induced cell cycle arrest in G0/G1 Phase

After the observation of the impact of As_2S_2 on the viability of SMMC-7721 cells, we examined the effect of As_2S_2 on cell cycle distribution of this cell line using FCM. The obtained results revealed that As_2S_2 induced a remarkable cell cycle arrest in G0/G1 phase. Cells at G0/G1 phase increased from 42.9 to 60.7% when treated with 50 μM As_2S_2 for 24 h (Fig. 1d, e).

As_2S_2 induced apoptosis in SMMC-7721 cells

Blocking cell cycle could induce apoptosis, after being treated with As_2S_2, SMMC-7721 cells were dyed with Annexin V/PI, then analyzed using FCM. As shown in Fig. 2a, As_2S_2 induced apoptosis in a concentration-dependent manner in SMMC-7721 cells. The percentage of apoptosis were increased by 12.92, 40.66 and 49.33% when SMMC-7721 cells were treated with 12.5, 25 and 50 mM of As_2S_2 for 24 h (Fig. 2b). For qualitative analysis of live and dead cells we used Calcein-AM and PI simultaneous fluorescence staining. As shown in Fig. 2c, d, the control cells glowed green fluorescence, meaning they were alive. The living cells in the control group were polygonal or spindle shaped, and the cells in the As_2S_2 groups became round. Dead cells dyed by PI with a red fluorescence were observed, and cells treated with As_2S_2 increased significantly by comparison with the untreated control group. Hoechst 33258 staining was used to evaluate whether As_2S_2 induced reduction in SMMC-7721 cell viability was responsible for the induction of apoptosis (Fig. 2e, f). After staining with Hoechst 33258, different degrees of growth inhibition and nuclear apoptotic bodies were observed in SMMC-7721 cells detected by a blue fluorescence staining of nuclei. These results showed that most of the cell death induced by As_2S_2 could be classified as apoptosis and As_2S_2 induced apoptosis through a dose-dependent manner.

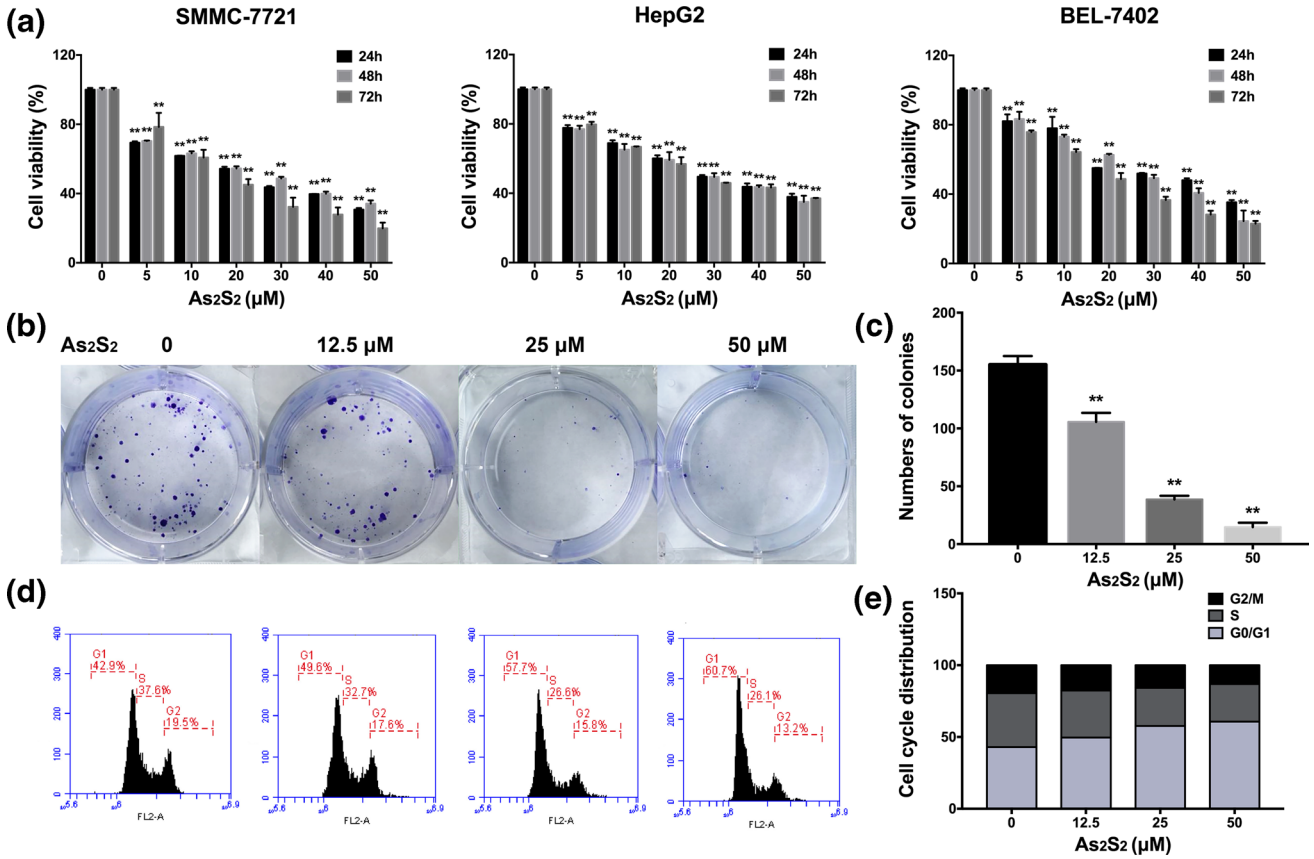

Fig. 1 As_2S_2 inhibited the cell viability in human liver cancer cell lines, inhibited colony formation and G0/G1 cell cycle arrest in SMMC-7721 cells. **a** SMMC-7721, BEL-7402, HepG2 cells were treated with indicated concentrations of As_2S_2 for 24, 48 or 72 h. Cell viability was measured by CCK-8. **b, c** SMMC-7721 cells were treated with As_2S_2 (0, 12.5, 25, 50 μM) for 14 days and colony formation was evaluated by crystal violet staining. **d, e** Cell cycle distribution was analyzed by FCM. SMMC-7721 cells were treated with different concentrations of As_2S_2 (0, 12.5, 25 and 50 μM) for 24 h. $^{**}P < 0.01$, compared to control group

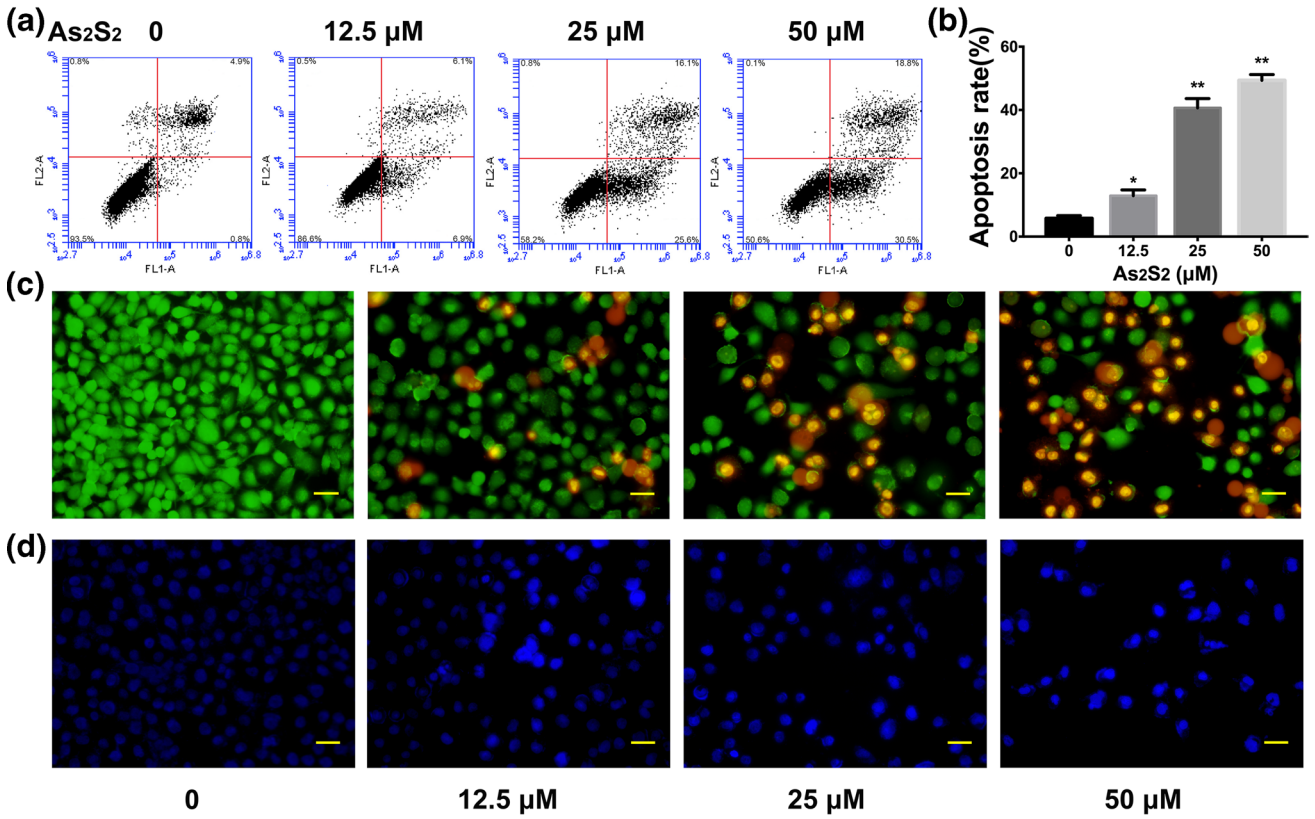

Fig. 2 As_2S_2 induced apoptosis in SMMC-7721 cells. **a, b** FCM analysis using Annexin V/PI staining was to identify apoptosis induced by As_2S_2. SMMC-7721 cells were treated with As_2S_2 for 24 h. **c** Live and dead cells were observed by Calcein-AM and PI double staining after treatment with As_2S_2 for 24 h. Scale bars represent 50 μm. **d** Quantification of live cells. **e** Hoechst 33258 staining of SMMC-7721 cells treated with As_2S_2 for 24 h. Scale bars represent 50 μm. **f** Quantification of apoptotic cells. $^*P<0.05$, $^{**}P<0.01$, compared to control group

As_2S_2 induced mitochondrial dysfunction in SMMC-7721 cells

To observe changes of the mitochondrial membrane potential of SMMC-7721 cells, JC-1 staining was applied to cells after As_2S_2 treatment. JC-1 aggregated in the mitochondria of normal cells to form a polymer that emitted red fluorescence. Once the mitochondrial membrane potential decreased, JC-1 mainly existed in the cytoplasm and emitted green fluorescence in the form of monomers.

As shown in Fig. 3a, images of fluorescence microscopy showed that red fluorescence decreased and green fluorescence increased markedly after As_2S_2 treatment for 24 h. There was a dose-dependent increase of green/red fluorescence intensity after treatment with 12.5, 25 and 50 μM of As_2S_2 for 24 h, and the ratios of green/red intensities were 1.34, 1.57 and 1.91, respectively (Fig. 3b). These results indicated that As_2S_2 could increase mitochondrial membrane permeability and lead to dysfunction of mitochondrial function in SMMC-7721 cells, revealing that As_2S_2 induced apoptosis in SMMC-7721 cells through the mitochondrial pathway.

As_2S_2 regulated the expression of apoptosis-related proteins in SMMC-7721 cells

To investigate the potential mechanisms of As_2S_2 induced apoptosis, Western blotting was applied to measure the expression of apoptosis-related proteins in SMMC-7721 cells. After exposure to As_2S_2 for 24 h, cytochrome *c* in mitochondria decreased while cytochrome *c* increased in the cytoplasm (Fig. 3c, d). After treatment with As_2S_2 for 24 h, the expression level of cleaved caspase-3 and PARP were increased. Meanwhile, the expression of pro-apoptotic protein Bax was increased while the anti-apoptotic protein Bcl-2 was suppressed by As_2S_2 (Fig. 3e–g). The above results indicated that As_2S_2 induced apoptosis probably via the mitochondrial-mediated apoptotic pathway in SMMC-7721 cells.

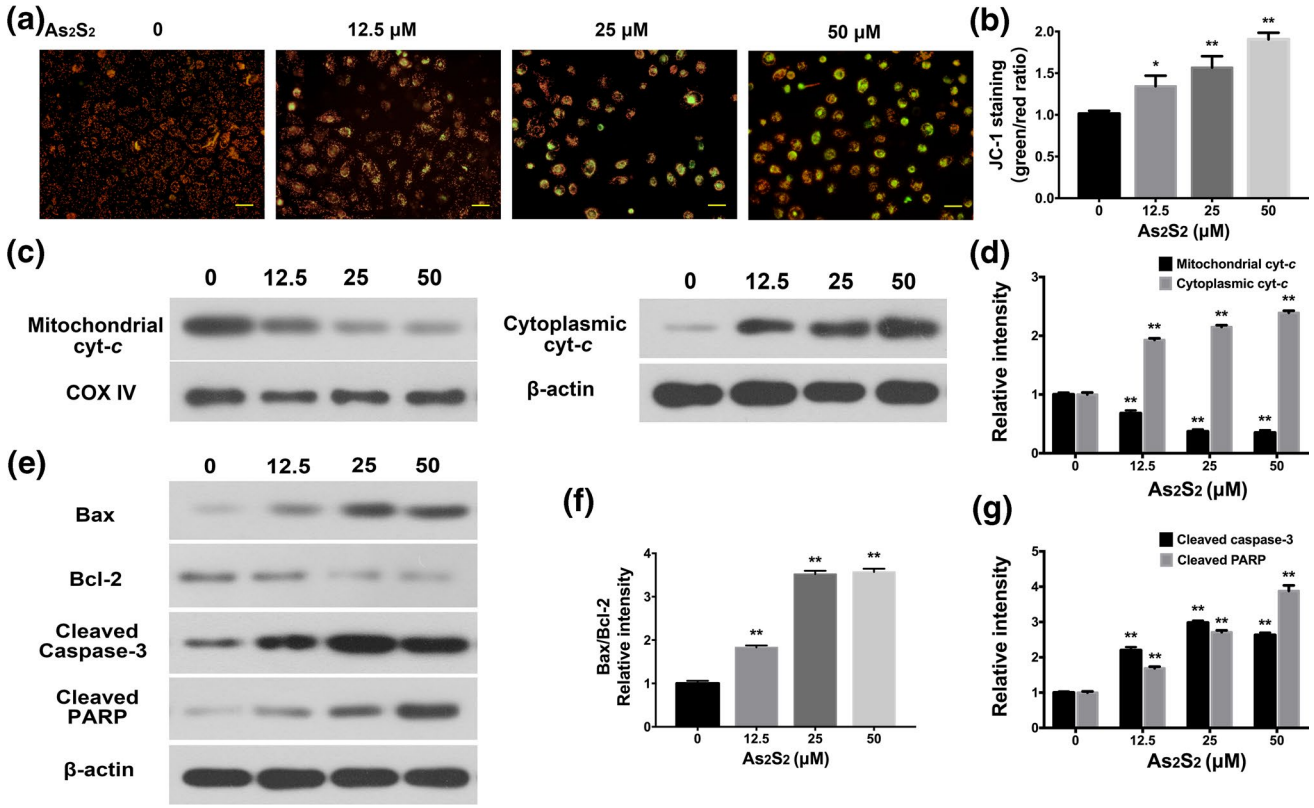

Fig. 3 As_2S_2 induced mitochondrial apoptosis in SMMC-7721 cells. **a** Cells were treated with As_2S_2 (0, 12.5, 25 and 50 μM) for 24 h, stained with JC-1 and observed under fluorescence microscope. Scale bars represent 50 μm. **b** Quantitative analysis of green/red fluorescence in SMMC-7721 cells. **c, d** Cytochrome *c* protein levels in the mitochondria and cytoplasm. **e–g** Regulative effects of As_2S_2 on Bax, Bcl-2, Cleaved Caspase-3, Cleaved PARP. β-Actin and COX IV were used as the loading control. $^*P<0.05$, $^{**}P<0.01$, compared to control group

As_2S_2 induced apoptosis through PI3K/AKT-mediated mitochondrial pathways in SMMC-7721 cells

As one of the important signal transduction pathways in cells, PI3K/AKT signaling pathway acts a pivotal role in suppressing apoptosis and enhancing proliferation by influencing the activation status of a variety of effector molecules downstream [26]. To explore the effect of As_2S_2 on PI3K/AKT pathway in SMMC-7721 cells, Western blotting was applied to detect the expression levels of PI3K/AKT after treatment of As_2S_2 for 24 h. As in Fig. 4a–c, the phosphorylation of PI3K and AKT was significantly decreased, and with the increase of the concentration of As_2S_2, the inhibition effect was more obvious. We used LY294002 (PI3K specific inhibitor) to pretreat SMMC-7721 cells to detect the role of PI3K/AKT pathway in As_2S_2-induced apoptosis. Compared with the control cells, 25 and 50 μM LY294002 could significantly reduce the expression of p-PI3K, p-AKT and regulate the expression of apoptosis-related proteins. While the simultaneous treatment of 25 μM LY294002 and 25 μM As_2S_2 could also play the same role, there were significant differences with 25 μM LY294002 or As_2S_2 treatment alone (Fig. 4d–g). These results suggested that PI3K/AKT-mediated mitochondrial pathways participated in As_2S_2-induced apoptosis.

As_2S_2 antineoplasmic activity in H22-bearing mice

To discuss the role of As_2S_2 on tumor growth, we established the model of H22-bearing mice. Compared to the model group, tumor weights of As_2S_2 treated groups decreased significantly ($P<0.01$). After treatment with As_2S_2 for 12 days, there was no significant difference in weight growth between the treatment groups (Fig. 5a), as shown in Fig. 5b, tumor growth inhibition in 5-Fu group (25 mg/kg), high-dose group (3.2 mg/kg), medium-dose group (1.6 mg/kg) and low-dose group (0.8 mg/kg) was 71.05, 53.51, 49.51 and 45.77%, respectively. To observe the pathological changes of tumors, we used HE staining. As shown in Fig. 5c, the tumor cells of the model group were heteromorphic, the volume of tumor cells increased, the ratio of nucleoplasm increased significantly, the ratio of

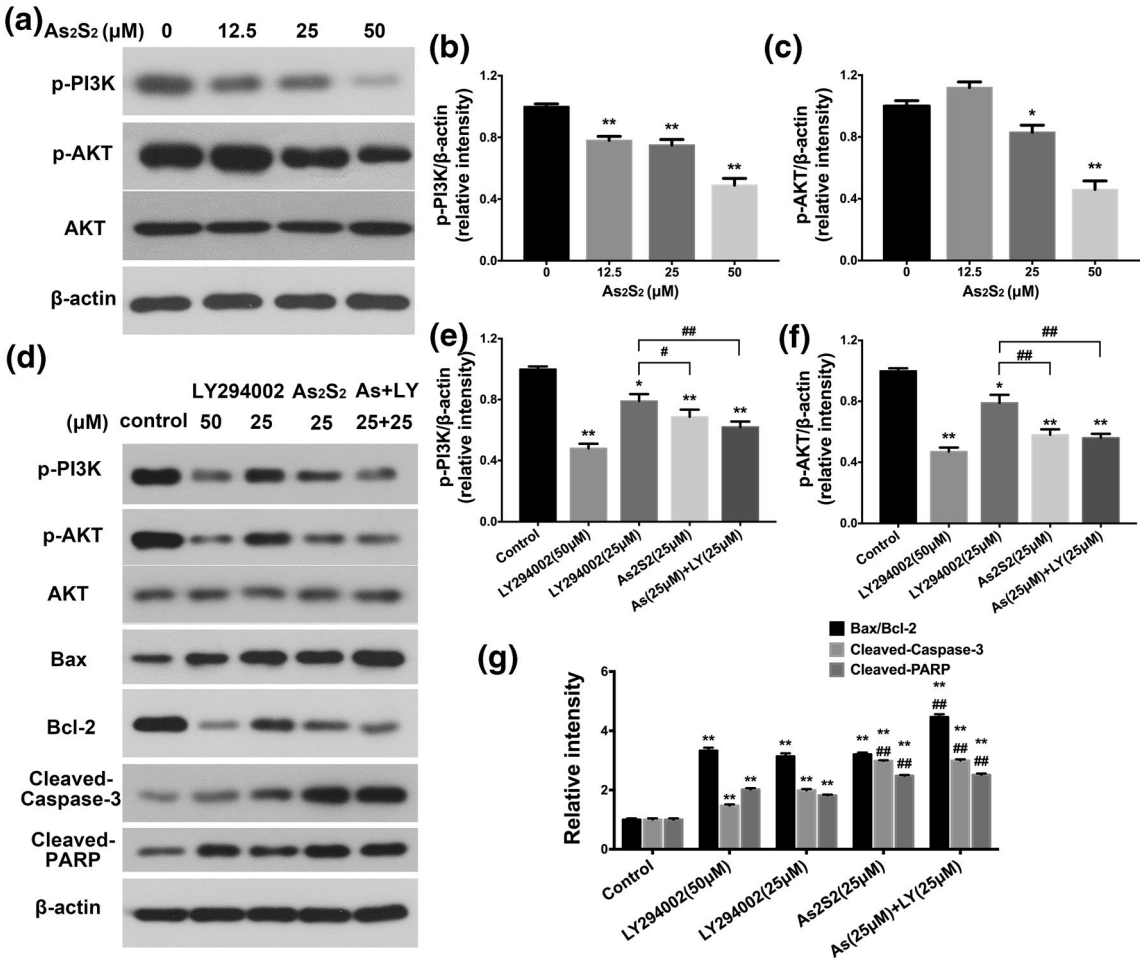

Fig. 4 Effects of As_2S_2 on the expression of PI3K/AKT-mediated mitochondrial pathway. SMMC-7721 cells were treated with various concentrations of As_2S_2 (0, 12.5, 25 and 50 μM) for 24 h. **a**–**c** The protein levels of phosphorylation of PI3K and AKT were determined by Western blot analysis. **d**–**g** Western blot analysis of PI3K/AKT-mediated mitochondrial pathway proteins, including Bax, Bcl-2, cleaved caspase-3 and PARP. β-Actin was used as loading control. $^{*}P<0.05$, $^{**}P<0.01$, compared to control group, $^{\#}P<0.05$, $^{\#\#}P<0.01$, compared to 25 μM LY294002

nucleoplasm was imbalanced and inflammatory cell infiltration was found. However, the tumor cells of 5-Fu, As_2S_2 groups showed varying degrees of apoptosis. We used immunohistochemical staining of PCNA to evaluate the the impact on cell proliferation of As_2S_2. As shown in Fig. 5d, compared with the model group, the number of PCNA-positive cells reduced significantly. Quantitative analysis showed that As_2S_2-treated groups could inhibit cell proliferation in a dose-dependent manner (Fig. 5f). Moreover, to explore whether As_2S_2 could induce apoptosis in H22-bearing mice, we used TUNEL assay to detect it by fluorescence microscopy. Compared with the model group, the number of TUNEL-positive cells increased significantly, indicating that As_2S_2-treated groups could promote cell apoptosis (Fig. 5e, g). These results were consistent with in vitro results, suggesting that the anti-tumor effect of As_2S_2 may be caused by apoptosis.

To illustrate the mechanisms of As_2S_2 resistance to H22-bearing mice, we detected the expression and phosphorylation of PI3K, AKT, Bax, Bcl-2 via Western blotting. As shown in Fig. 5h, i, compared with the model group, the phosphorylation of AKT and PI3K was decreased in tumors of H22-bearing mice treated with As_2S_2, significantly. These results indicated that PI3K/AKT signaling pathway might be involved in As_2S_2-treated tumors of H22-bearing mice.

Discussion

Liver cancer is one of the most frequent, malignant neoplasms worldwide, and for decades, the incidence and mortality of liver cancer have gradually increased [27]. Surgery, local destructive treatment and liver transplantation are available medical measures for patients with early liver

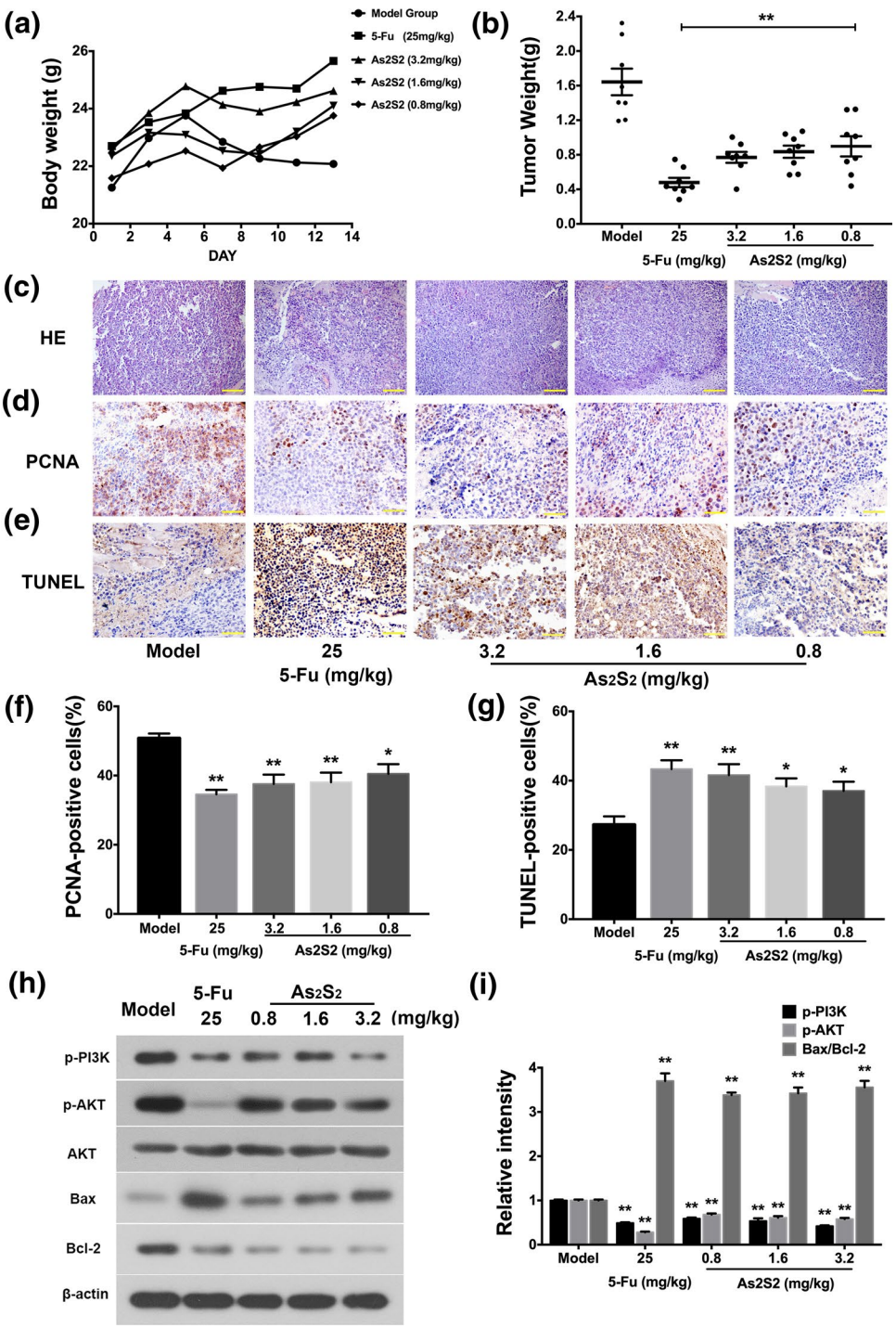

Fig. 5 As_2S_2 inhibited the growth of tumors in H22-bearing mice. **a** Body weights of mice were recorded every 2 days. **b** The mean tumor weights of mice in different groups. **c** Histopathological observation of tumor in different groups (HE staining; magnification, ×200). Scale bars represent 100 μm. **d** Immunohistochemistry for PCNA (magnification, ×400). Scale bars represent 50 μm. **e** Detection of apoptotic cells by TUNEL (magnification, ×400). Scale bars represent 50 μm. **f** The percentage of PCNA-positive cells. **g** The percentage of TUNEL-positive cells. **h, i** The protein of phosphorylation of PI3K and AKT, Bax, Bcl-2 were detected by Western blot analysis. $^*P<0.05$, $^{**}P<0.01$, compared to model group

cancer. In addition, radiotherapy and chemotherapy also have certain effect on liver cancer patients, but constant side effects make patients miserable [28]. Hence, it is of great significance to develop new therapeutic agents for liver cancer to relieve patients' pain and improve their quality of life.

TCM has shown its unique advantages and has proved to be effective in anti-cancer [29]. At present, research on anti-tumor activity of mineral arsenicals in traditional medicines has become a hot topic. As_2S_2 is the main effective component from the realgar of traditional Chinese mineral medicine, which has been applied to treat various diseases for thousands of years. Good antitumor effect of As_2S_2 has been confirmed, particularly for hematological malignancies, and the ability of As_2S_2 to induce apoptosis in several solid tumors has also been demonstrated [30–34]. The effect of As_2S_2 in liver cancer has rarely been reported;

therefore, its role in the treatment of liver cancer needs to be further elaborated. In the present study, we investigated the antitumor effect of As_2S_2 on liver cancer and its potential mechanism of action in vivo and in vitro.

In the current study, we found that As_2S_2 could significantly inhibit the proliferation of human hepatoma cell lines SMMC-7721, BEL-7402 and HepG2 via CCK-8 assay, and the IC_{50} value were 25.63 ± 1.05, 28.99 ± 3.44 and 30.15 ± 3.43 μM after treatment of As_2S_2 for 24 h in vitro (Fig. 1a). Subsequent experimental results revealed that As_2S_2 significantly restrained the colony formation in SMMC-7721 cells and presented a concentration-dependent relationship (Fig. 1b, c), which was mainly due to the blocking of cells at G0/G1 phase and inducing apoptosis. The process of cell cycle dominates cell proliferation, and its imbalance is one of the critical stages of cancer development [35]. Accordingly, regulating cell cycle progression by stalling the cell cycle may be an appropriate treatment for cancer. FCM analysis stated clearly that compared with control cells, As_2S_2-treated SMMC-7721 cells apparently accumulated in G0/G1 phase, while S phase and G2/M phase decreased correspondingly (Fig. 1d, e). These results showed that As_2S_2 inhibited cell proliferation in a concentration-dependent manner by blocking cells at the G0/G1 phase, and the G1/S checkpoint prevents cells from passing through G1 phase into the S phase of DNA synthesis.

Cell cycle arrest and apoptosis induction are two concernment accounts to inhibit the growth and proliferation of tumor cells [36]. In our research, Annexin V-FITC/PI staining FCM analysis results represented that the apoptotic rates of SMMC-7721 cells concentration-dependently increased with As_2S_2 treatment (Fig. 2a, b). Apoptotic cells exhibit unique morphology during the process of apoptosis, such as cell surface changes, DNA fragmentation, nuclear condensation and chromosome agglutination [37]. By Calcein-AM/PI staining and Hoechst 33258 staining, the number of As_2S_2-treated SMMC-7721 cells significantly decreased and showed typical apoptotic characteristics (Fig. 2c, d). These results indicated that As_2S_2 inhibited tumor cell proliferation by significantly inducing apoptotic cell death.

Apoptosis is tightly regulated by multiple genes, mainly containing two kinds of signal transduction pathways: death receptor-mediated exogenous apoptosis pathway and mitochondria-mediated endogenous apoptosis pathway [38]. Mitochondria are not only the energy supply center to maintain cell growth and division, but also exert a pivotal role in endogenous apoptosis pathway and are the ultimate regulator of apoptosis [39]. The mPTP located between the inner and outer mitochondrial membrane is one of the factors that affect transmembrane potential. After receiving apoptotic signals, the opening of mPTP channels directly leads to the decrease or even loss of transmembrane potential, which destroys the structure of inner and outer membrane and finally disintegrates mitochondria [40]. In our results, JC-1 staining revealed that mitochondrial membrane potential collapsed (Fig. 3a). Bcl-2 family proteins are the major regulators of mitochondrial-dependent apoptosis. They are membrane integrins belonging to the oncogene family, which exist in mitochondria, endoplasmic reticulum and cell nuclear membrane. Disproportionality of Bax/Bcl-2 leads to permeabilization of the outer mitochondrial membrane, thereby releasing cytochrome *c* to cytosol, activating caspases-3, and ultimately inducing apoptosis [41]. Caspase-3 is the most significant apoptotic executor of the caspase family, responsible for the action of the enzyme (activation or inactivation) of all or part of the key proteins at the stage of apoptosis [42]. In this study, Western blot analysis demonstrated that As_2S_2 increased the Bax expression and decreased Bcl-2 expression (Fig. 3d, e). The rise in Bax/Bcl-2 ratio led to the intrinsic pathway of depolarization activation of mitochondrial membrane potential, which resulted in cytochrome *c* release; the caspase-3 precursor protein was cut into the activated caspase-3, and the damage repair sensing molecule PARP was deactivated. As_2S_2 released cytochrome *c* from the lumen between the inner and outer membranes of the mitochondria into the cytoplasm (Fig. 3b, c) and increased the levels of cleaved caspase-3 and PARP in a concentration-dependent manner (Fig. 3d, f), ultimately leading to apoptotic cell death. These results demonstrated that As_2S_2 could induce apoptosis of SMMC-7721 cells through mitochondrial-mediated apoptosis pathway.

PI3K/AKT signaling pathway, as an important signaling pathway to regulate cell survival and apoptosis, has been proved to be overexpressed and activated in various cancers [43]. PI3K/AKT pathway is closely related to the activity of Bcl-2 family proteins, regulating metastasis progression and blocking apoptosis by phosphorylating apoptotic proteins and preventing the release of mitochondrial cytochrome *c*. Therefore, activation of PI3K/AKT pathway is carcinogenic, which is due to cell cycle disorder and the stimulation of anti-apoptotic pathway, and activated AKT promotes the resistance of cancer cells to apoptosis [44]. At present, blocking the activation of a variety of anti-apoptotic molecules in the PI3K/AKT pathway and promoting apoptosis have become the focus of cancer treatment. In the present study, As_2S_2-treatment decreased the expression level of p-PI3K and p-AKT significantly and regulated the expression of apoptosis-related proteins (Fig. 4a–c). It could be said that As_2S_2 and 25 μM LY294002 inhibited the expression of phosphorylated PI3K and AKT, activated the pro-apoptotic target Bax, inhibited the expression of Bcl-2, and the caspase-3 and PARP were deactivated that eventually led to apoptosis (Fig. 4d–g). The above results showed that As_2S_2 promoted the apoptosis via PI3K/AKT-mediated mitochondrial pathways of SMMC-7721 human hepatoma cells.

To evaluate the antitumor effect of As_2S_2 on liver cancer in vivo, BALB/c mice were ectopic inoculated with H22 murine tumor cells. In the selection of animal models and tumor cells in vivo, we chose H22-bearing mice model, which is widely and authoritatively established in the animal models of liver cancer, and the H22 cells are mouse-derived cells, it is more suitable for the model of liver cancer in mice [45]. We verified the effect of As_2S_2 on tumor weight reduction in mice. As_2S_2 could reduce the average tumor weight, and the tumor inhibition rates of different concentrations of As_2S_2 (3.2, 1.6 and 0.8 mg/kg) were, respectively, 53.51, 49.51 and 45.77%. Our results indicated that As_2S_2 was remarkably effective for inhibiting tumor growth (Fig. 5b) in a concentration-dependent manner and had no significant effect on body weight in mice (Fig. 5a). The results of immunohistochemical staining and TUNEL assay revealed that As_2S_2 suppressed tumor growth by inhibiting cell proliferation and inducing tumor cell apoptosis (Fig. 5d–g). The results of Western blot showed that As_2S_2 could down-regulate Bcl-2 and up-regulate Bax (Fig. 5h, i), indicating that the anti-tumor effect of As_2S_2 was achieved by inducing apoptosis. Simultaneously, treatment of As_2S_2 down-regulated the phosphorylation of PI3K and AKT (Fig. 5h, i), indicating that As_2S_2 induced apoptosis via inhibition of PI3K/AKT pathway in vivo, which was consistent with those obtained in vitro.

In conclusion, our results demonstrated that As_2S_2 induced apoptosis of liver cancer cells both in vivo and in vitro through PI3K/AKT-mediated mitochondrial pathway. These data indicated that As_2S_2 may be a promising anti-cancer drug for the treatment of malignant solid tumors.

Funding This study was funded by the National Natural Science Foundation of China (Nos. 81273883).

Compliance with ethical standards

Conflict of interest Author Shudan Wang declares that she has no conflict of interest. Author Chao Zhang declares that he has no conflict of interest. Author Yumei Li declares that she has no conflict of interest. Ping Li declares that she has no conflict of interest. Author Dafang Zhang declares that he has no conflict of interest. Author Chaoying Li declares that she has no conflict of interest.

Ethical approval All applicable national and institutional guidelines for the care and use of animals were followed. This article does not contain any studies with human participants performed by any of the authors.

References

1. Sia D, Villanueva A, Friedman SL, Llovet JM (2017) Liver cancer cell of origin, molecular class, and effects on patient prognosis. Gastroenterology 152(4):745–761. https://doi.org/10.1053/j.gastro.2016.11.048
2. Jemal A, Bray F, Center MM, Ferlay J, Ward E, Forman D (2011) Global cancer statistics. CA Cancer J Clin 61(2):69–90. https://doi.org/10.3322/caac.20107
3. Wu Z, Wu J, Fang P, Kan SF (2017) Puerarin increases the chemosensitivity of hepatocellular carcinoma cells. Oncol Lett 14(3):3006–3010. https://doi.org/10.3892/ol.2017.6524
4. Khiewkamrop P, Phunsomboon P, Richert L, Pekthong D, Srisawang P (2018) Epistructured catechins, EGCG and EC facilitate apoptosis induction through targeting de novo lipogenesis pathway in HepG2 cells. Cancer Cell Int 18:46. https://doi.org/10.1186/s12935-018-0539-6
5. Zi D, Zhou ZW, Yang YJ, Huang L, Zhou ZL, He SM, He ZX, Zhou SF (2015) Danusertib induces apoptosis, cell cycle arrest, and autophagy but inhibits epithelial to mesenchymal transition involving PI3K/AKT/mTOR signaling pathway in human ovarian cancer cells. Int J Mol Sci 16(11):27228–27251. https://doi.org/10.3390/ijms161126018
6. Wang CH, Lu SX, Liu LL, Li Y, Yang X, He YF, Chen SL, Cai SH, Wang H, Yun JP (2018) POH1 knockdown induces cancer cell apoptosis via p53 and Bim. Neoplasia 20(5):411–424. https://doi.org/10.1016/j.neo.2018.02.005
7. Antoniou N, Vlachakis D, Memou A, Leandrou E, Valkimadi PE, Melachroinou K, Re DB, Przedborski S, Dauer WT, Stefanis L, Rideout HJ (2018) A motif within the armadillo repeat of Parkinson's-linked LRRK2 interacts with FADD to hijack the extrinsic death pathway. Sci Rep 8(1):3455. https://doi.org/10.1038/s41598-018-21931-8
8. Jiao HL, Guan FX, Yang B, Li JB, Song LJ, Hu X, Du Y (2012) Human amniotic membrane derived- mesenchymal stem cells induce C6 glioma apoptosis in vivo through the Bcl-2/caspase pathways. Mol Biol Rep 39(1):467–473. https://doi.org/10.1007/s11033-011-0760-z
9. Niknejad H, Khayat-Khoei M, Peirovi H, Abolghasemi H (2014) Human amniotic epithelial cells induce apoptosis of cancer cells: a new anti-tumor therapeutic strategy. Cytotherapy 16(1):33–40. https://doi.org/10.1016/j.jcyt.2013.07.005
10. Wang J, Yuan L, Xiao HF, Xiao CX, Wang YT, Liu XB (2013) Momordin Ic induces HepG2 cell apoptosis through MAPK and PI3K/AKT-mediated mitochondrial pathways. Apoptosis 18:751–765. https://doi.org/10.1007/s10495-013-0820-z
11. Gerisch M, Schwarz T, Lang D, Rohde G, Reif S, Genvresse I, Reschke S, van der Mey D, Granvil C (2017) Pharmacokinetics of intravenous pan-class I phosphatidylinositol 3-kinase (PI3K) inhibitor [^{14}C] copanlisib (BAY 80-6946) in a mass balance study in healthy male volunteers. Cancer Chemother Pharmacol 80(3):535–544. https://doi.org/10.1007/s00280-017-3383-9
12. Zhang C, Li CW, Chen SH, Li ZP, Jia XJ, Wang K, Bao JL, Liang Y, Wang XT, Chen MW, Li P, Su HX, Wan JB, Lee SMY, Liu KC, He CW (2017) Berberine protects against 6-OHDA-induced neurotoxicity in PC12 cells crossmark and zebrafish through hormetic mechanisms involving PI3K/AKT/Bcl-2 and Nrf2/HO-1 pathways. Redox Biol 11:1–11. https://doi.org/10.1016/j.redox.2016.10.019
13. Youle RJ, Strasser A (2008) The BCL-2 protein family: opposing activities that mediate cell death. Nat Rev Mol Cell Biol 9(1):47–59. https://doi.org/10.1038/nrm2308
14. Parcellier A, Tintignac LA, Zhuravleva E, Hemmings BA (2008) PKB and the mitochondria: AKTing on apoptosis. Cell Signal 20(1):21–30. https://doi.org/10.1016/j.cellsig.2007.07.010
15. Li XQ, Lin ZH, Zhang B, Guo L, Liu S, Li H, Zhang JB, Ye QH (2016) β-elemene sensitizes hepatocellular carcinoma cells to oxaliplatin by preventing oxaliplatin-induced degradation of copper transporter 1. Sci Rep 6:21010. https://doi.org/10.1038/srep21010
16. Wang XB, Wang N, Cheung F, Lao LX, Li C, Feng YB (2015) Chinese medicines for prevention and treatment of human

hepatocellular carcinoma: current progress on pharmacological actions and mechanisms. J Integr Med 13(3):142–164. https://doi.org/10.1016/S2095-4964(15)60171-6
17. Khairul I, Wang QQ, Jiang YH, Wang C, Naranmandura H (2017) Metabolism, toxicity and anticancer activities of arsenic compounds. Oncotarget 8(14):23905–23926. https://doi.org/10.18632/oncotarget.14733
18. Lo-coco F, Avvisati G, Vignetti M et al (2013) Retinoic acid and arsenic trioxide for acute promyelocytic leukemia. N Engl J Med 369(2):111–121. https://doi.org/10.1056/NEJMoa1300874
19. Hughes MF (2002) Arsenic toxicity and potential mechanisms of action. Toxicol Lett 133(1):1–7. https://doi.org/10.1016/S0378-4274(02)00084-X
20. Zhang L, Tian W, Kim S, Ding WP, Tong YY, Chen SY (2014) Arsenic sulfide, the main component of realgar, a traditional Chinese medicine, induces apoptosis of gastric cancer cells in vitro and in vivo. Drug Des Dev Ther 9:79–92. https://doi.org/10.2147/DDDT.S74379
21. Wang GY, Zhang T, Sun W, Wang HS, Yin F, Wang ZY, Zuo DQ, Sun MX, Zhou ZF, Lin BH, Xu J, Hua YQ, Li HQ, Cai ZD (2017) Arsenic sulfide induces apoptosis and autophagy through the activation of ROS/JNK and suppression of AKT/mTOR signaling pathways in osteosarcoma. Free Radic Bio Med 106:24–37. https://doi.org/10.1016/j.freeradbiomed.2017.02.015
22. Xu M, Ren JY, Guo YC, Xu BX, Zeng Q, Hu Q, Zhou YM, Lu JH (2017) Effects of arsenic disulfide on apoptosis, histone acetylation, toll like receptor 2 activation, and erythropoiesis in bone marrow mononuclear cells of myelodysplastic syndromes patients in vitro. Leuk Res 62:4–11. https://doi.org/10.1016/j.leukres.2017.09.010
23. Zhang XL, Kang T, Zhang L, Tong Y, Ding W, Chen S (2017) NFATc3 mediates the sensitivity of gastric cancer cells to arsenic sulfide. Oncotarget 8(32):52735–52745. https://doi.org/10.18632/oncotarget.17175
24. Song P, Hai Y, Wang X, Zhao LH, Chen BQ, Cui P, Xie QJ, Yu L, Li Y, Wu ZG, Li HY (2018) Realgar transforming solution suppresses angiogenesis and tumor growth by inhibiting VEGF receptor 2 signaling in vein endothelial cells. Arch Pham Res 41(4):467–480. https://doi.org/10.1007/s12272-018-1014-6
25. Perelman A, Wachtel C, Cohen M, Haupt S, Shapiro H, Tzur A (2012) JC-1: alternative excitation wavelengths facilitate mitochondrial membrane potential cytometry. Cell Death Dis 3:e430. https://doi.org/10.1038/cddis.2012.171
26. Xu C, Sun GB, Yuan GX, Wang R, Sun XB (2014) Effects of platycodin D on proliferation, apoptosis and PI3K/Akt signal pathway of human glioma U251 cells. Molecules 19(12):21411–21423. https://doi.org/10.3390/molecules191221411
27. Altekruse SF, Henley SJ, Cucinelli JE, McGlynn KA (2014) Changing hepatocellular carcinoma incidence and liver cancer mortality rates in the United States. Am J Gastroenterol 109(4):542–553. https://doi.org/10.1038/ajg.2014.11
28. Liu CY, Chen KF, Chen PJ (2015) Treatment of liver cancer. Cold Spring Harb Perspect Med 5(9):a021535. https://doi.org/10.1101/cshperspect.a021535
29. Gao L, Wang XD, Niu YY, Duan DD, Yang X, Hao J, Zhu CH, Chen D, Wang KX, Qin XM, Wu XZ (2016) Molecular targets of Chinese herbs: a clinical study of hepatoma based on network pharmacology. Sci Rep 6:24944. https://doi.org/10.1038/srep24944
30. He PC, Liu YF, Qi J, Zhu HC, Wang Y, Zhao J, Cheng XY, Wang C, Zhang M (2015) Prohibitin promotes apoptosis of promyelocytic leukemia induced by arsenic sulfide. Int J Oncol 47(6):2286–2295. https://doi.org/10.3892/ijo.2015.3217
31. Lu DP, Qiu JY, Jiang B, Wang Q, Liu KY, Liu YR, Chen SS (2002) Tetra-arsenic tetra-sulfide for the treatment of acute promyelocytic leukemia: a pilot report. Blood 99:3136–3143. https://doi.org/10.1182/blood.V99.9.3136
32. Ding WP, Tong YY, Zhang XL, Pan MG, Chen SY (2016) Study of arsenic sulfide in solid tumor cells reveals regulation of nuclear factors of activated T-cells by PML and p53. Sci Rep 6:19793. https://doi.org/10.1038/srep19793
33. Zhang L, Tong YY, Zhang XL, Pan MG, Chen S (2015) Arsenic sulfide combined with JQ1, chemotherapy agents, or celecoxib inhibit gastric and colon cancer cell growth. Drug Des Devel Ther 9:5851–5862. https://doi.org/10.2147/DDDT.S92943
34. Zhang L, Kim S, Ding WP, Tong YY, Zhang XL, Pan MG, Chen SY (2015) Arsenic sulfide inhibits cell migration and invasion of gastric cancer in vitro and in vivo. Drug Des Devel Ther 9:5579–5590. https://doi.org/10.2147/DDDT.S89805
35. Li X, Qiu ZD, Jin QH, Chen GL, Guo MQ (2018) Cell cycle arrest and apoptosis in HT-29 cells induced by dichloromethane fraction from *Toddalia asiatica* (L.) Lam. Front Pharmacol 9:629. https://doi.org/10.3389/fphar.2018.00629
36. Zhao YX, Yuan B, Onda K, Sugiyama K, Tanaka S, Takagi N, Hirano T (2018) Anticancer efficacies of arsenic disulfide through apoptosis induction, cell cycle arrest, and pro-survival signal inhibition in human breast cancer cells. Am J Cancer Res 8(3):366–386
37. Guo CL, Wang LJ, Zhao Y, Liu H, Li XQ, Jiang B, Luo J, Guo SJ, Wu N, Shi DY (2018) A novel bromophenol derivative BOS-102 induces cell cycle arrest and apoptosis in Human A549 lung cancer cells via ROS-mediated PI3K/AKT and the MAPK signaling pathway. Mar Drugs 16(2):43. https://doi.org/10.3390/md16020043
38. Yang CH, Cai H, Meng XX (2016) Polyphyllin D induces apoptosis and differentiation in K562 human leukemia cells. Int Immunopharmacol 36:17–22. https://doi.org/10.1016/j.intimp.2016.04.011
39. Kubli DA, Gustafsson ÅB (2012) Mitochondria and mitophagy: the yin and yang of cell death control. Circ Res 111(9):1208–1221. https://doi.org/10.1161/CIRCRESAHA.112.265819
40. Wang LL, Han L, Ma XL, Yu Q, Zhao SN (2017) Effect of mitochondrial apoptotic activation through the mitochondrial membrane permeability transition pore on yak meat tenderness during postmortem aging. Food Chem 234:323–331. https://doi.org/10.1016/j.foodchem.2017.04.185
41. Shi JJ, Jiang Q, Ding XW, Xu WH, Wang DW, Chen ML (2015) The ER stress-mediated mitochondrial apoptotic pathway and MAPKs modulate tachypacing-induced apoptosis in HL-1 atrial myocytes. PLoS One 10(2):e0117567. https://doi.org/10.1371/journal.pone.0117567
42. Shalini S, Dorstyn L, Dawar S, Kumar S (2015) Old, new and emerging functions of caspases. Cell Death Differ 22(4):526 –526 39. https://doi.org/10.1038/cdd.2014.216
43. Faes S, Dormond O (2015) PI3K and AKT: unfaithful partners in cancer. Int J Mol Sci 16(9):21138–21152. https://doi.org/10.3390/ijms160921138
44. Zhu JW, Sun Y, Lu Y, Jiang XB, Ma B, Yu LS, Zhang J, Dong XC, Zhang Q (2018) Glaucocalyxin A exerts anticancer effect on osteosarcoma by inhibiting GLI1 nuclear translocation via regulating PI3K/Akt pathway. Cell Death Dis 9(6):708. https://doi.org/10.1038/s41419-018-0684-9
45. Miao S, Wang MS, Cheng X, Li YF, Zhang QS, Li G, He QS, Chen XP, Wu P (2017) Erythropoietin promoted the proliferation of hepatocellular carcinoma through hypoxia induced translocation of its specific receptor. Cancer Cell Int 17: 119.https://doi.org/10.1186%2Fs12935-017-0494-7